World Academy of Science, Engineering and Technology
International Journal of Aerospace and Mechanical Engineering
Vol:12, No:8, 2018

Laser Beam Micro-Drilling Effect on Ti-6Al-4V Titanium Alloy Sheet Properties

Petr Homola, Roman Růžek

Open Science Index, Aerospace and Mechanical Engineering Vol:12, No:8, 2018 publications.waset.org/10009330/pdf

***Abstract*—**Laser beam micro-drilling (LBMD) is one of the most important non-contact machining processes of materials that are difficult to machine by means oeqf conventional machining methods used in various industries. The paper is focused on LBMD knock-down effect on Ti-6Al-4V (Grade 5) titanium alloy sheets properties. Two various process configurations were verified with a focus on laser damages in back-structure parts affected by the process. The effects of the LBMD on the material properties were assessed by means of tensile and fatigue tests and fracture surface analyses. Fatigue limit of LBMD configurations reached a significantly lower value between 15% and 30% of the static strength as compared to the reference raw material with 58% value. The farther back-structure configuration gives a two-fold fatigue life as compared to the closer LBMD configuration at a given stress applied.

***Keywords*—**Fatigue, fracture surface, laser beam micro-drilling, titanium alloy.

I. Introduction

THIS paper has been prepared in the framework of the AFLoNEXT (2nd Generation Active Wing - Active Flow, Loads & Noise control on next generation wing) European project No. 604013. AFLoNEXT aimed to prove the engineering feasibility of the hybrid laminar flow control (HLFC) technology for drag reduction on fin in flight test and on wing by means of large scale testing [1]. The project also showed engineering feasibility for vibrations mitigation technologies for reduced aircraft weight and noise mitigation technologies. To improve aircraft performance along the whole flight regime, locally applied active flow control technologies on wing and wing/pylon junction were qualified in wind tunnels or by means of lab-type demonstrators. 40 partners from 15 countries cooperated in this project.

The paper is a part of project technology stream focused on the HLFC on wing and fin. A HLFC wing leading-edge concept for a large passenger aircraft has been designed to enable significant drag reduction. The leading-edge concept includes a novel Krueger flap high-lift system, integrated suction, and hot air anti-icing air systems. The massive effort results in a 2.3 m span ground-based demonstrator (GBD), including the manufacturing of a super-plastically formed suction leading-edge panel. The effectiveness of a hot air anti-icing system has been demonstrated in an icing wind tunnel test. Fig. 1 shows scheme of wing GBD with developed Krueger flap and HLFC suction panel.

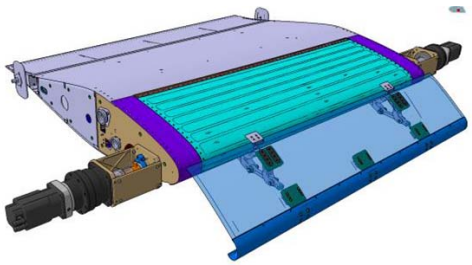


Fig. 1 Wing GBD with deployed Krueger flap [2]

The functionality of hot air anti-icing system was supported using the panels with LBMD holes. This applied technology has to ensure not only functionality, but also strength properties covering requirements of airworthiness regulations. The paper discusses influences of the micro drilling technology on static and fatigue properties of a titanium alloy.

II. Experimental

A. Materials

Ti-6Al-4V (Grade 5) titanium alloy sheets (Table I) of 0.6 and 1.0 mm in thickness were used for the experiments. The as-received sheets were in annealed condition (790 °C/50 min, air cooled).

TABLE I
Nominal Composition of the Experimental Material (wt.%)

Ti-6Al-4V	Al	V	Fe	C	N	H	O	Ti
Min.	5.5	3.5	–	–	–	–	–	–
Max.	6.8	4.5	0.3	0.08	0.05	0.01	0.2	bal.

LBMD process was performed and developed by SONACA. The influence of two different micro-drilling process configurations was evaluated on the following four batches (see Fig. 2):

- Reference blank sheet (designated as Ref), 1.0 mm thick;
- Micro-drilled (MD) sheet, 1.0 mm thick;
- Back-structure sheet at distance of 2.5 mm behind the MD surface (Int2.5), 0.6 mm thick;
- Back-structure sheet at distance of 12 mm behind the MD surface (Int12), 1.0 mm thick.

Detailed three dimensional micrographs showing an appearance of the top surface of the MD sheet and the back-structure sheets (Int2.5 and Int12) and the bottom surface (only in case of MD sheet) are presented in Fig. 3.

P. Homola is with the Czech Aerospace Research Centre, Beranovych 130, Prague, 195 00 Czech Republic (phone: +420 225 115 303; e-mail: homola@vzlu.cz).

R. Růžek is with the Czech Aerospace Research Centre, Beranovych 130, Prague, 195 00 Czech Republic.

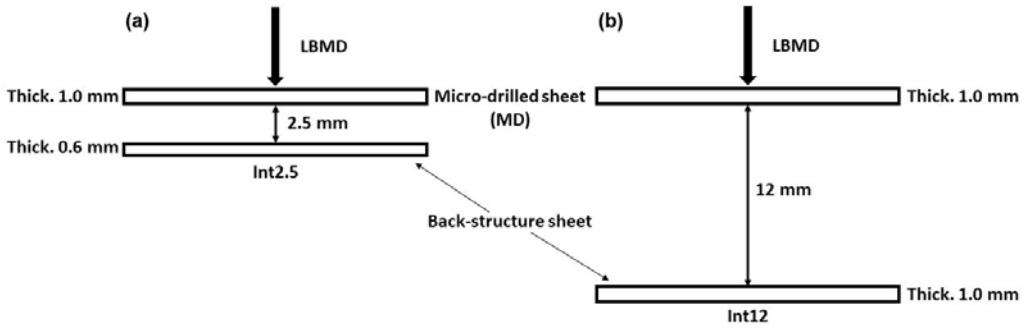


Fig. 2 Various micro-drilling configurations with back-structure sheet at distance of (a) 2.5 mm and (b) 12 mm behind LBMD surface

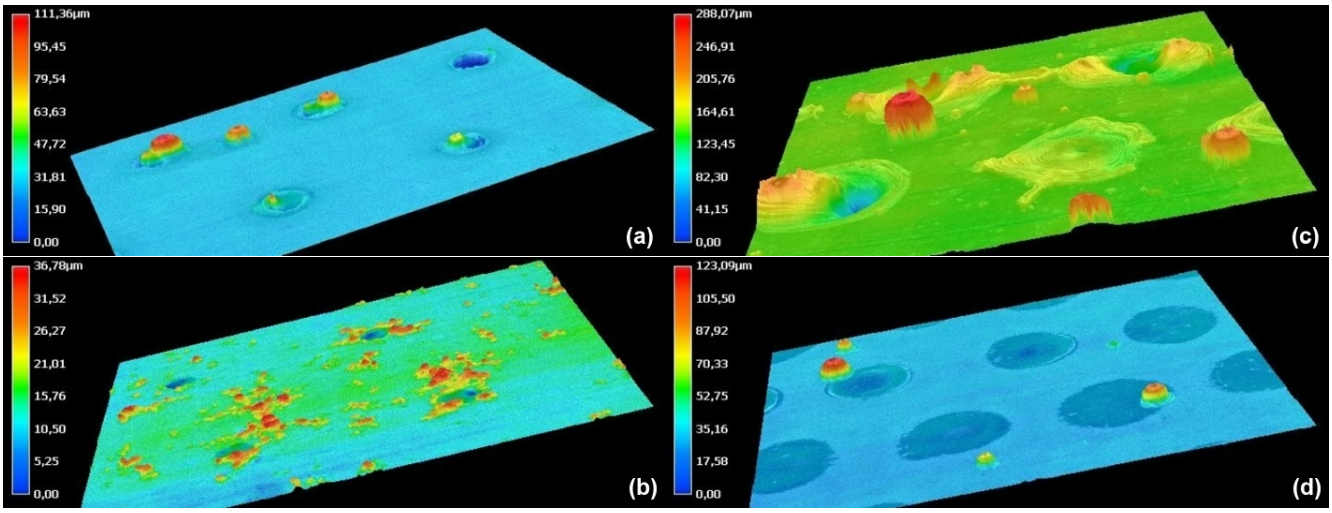


Fig. 3 3D micrographs with appearance of the top and bottom surface of the D) sheet (a,b) and the top surface of the back-structure sheets Int2.5 (c) and Int12 (d)

A. Experimental Methods

The tensile and fatigue test specimen geometries are shown in Fig. 4. Three and at least 15 test specimens cut in L-T direction were tested within the tensile and fatigue tests, respectively. The static tensile tests were carried out in accordance with the ISO 6892-1 standard [3] under displacement control at 1.1 mm/min cross-head speed with usage of an extensometer with a gage length of 50 mm.

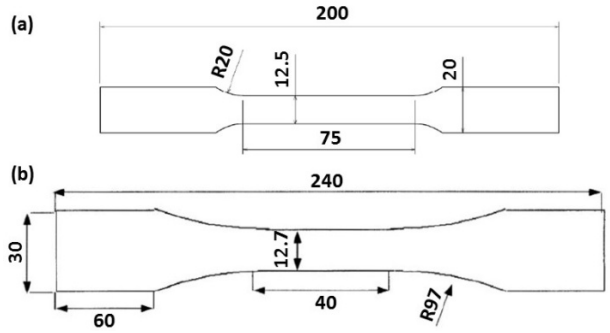


Fig. 4 The tensile (a) and fatigue (b) test specimen geometries

The fatigue tests were performed using a harmonic loading (sinusoidal load cycle) with a constant amplitude force range with the stress ratio of 0.1. Fatigue tests were conducted in accordance with procedures defined in EN 6072 standard [4]. The test frequencies in range of 15 – 20 Hz were used.

All static tensile and fatigue tests were performed at room temperature (23±2 °C) and under standard laboratory conditions.

3D micrographs (Fig. 3) showing the appearance of the top and bottom surface of individual processed sheets were made by means of the digital microscope Keyence VHX-6000 at a magnification of 1000× using a stitching image and depth composition method.

Fractographic analyses of selected fatigue test specimen's fracture surface were performed using the scanning electron microscope Vega 3SBU (Tescan) operating at 30 kV and using the secondary electron (SE) observation mode. The fracture surfaces of the selected fatigue test specimens for the fractographic analysis were cut by means of linear precision saw IsoMet 4000 using a blade speed of 3000 rpm and cutting rate of 2.5 mm/min.

III. Results and Discussion

A. Tensile Tests

Mean values of measured material characteristics (yield strength, ultimate strength and ductility) are summarized in Table II. The results in a graphical form are shown in Fig. 5.

Open Science Index, Aerospace and Mechanical Engineering Vol:12, No:8, 2018 publications.waset.org/10009330/pdf

Open Science Index, Aerospace and Mechanical Engineering Vol:12, No:8, 2018 publications.waset.org/10009330/pdf

TABLE II
TENSILE TESTS SUMMARY

Sheet type	Ref	MD	Int2.5	Int12
Yield strength $R_{p0.2}$ (MPa)	924.7	870.7	931.4	903.7
Ultimate strength R_m (MPa)	990.9	946.0	976.5	978.5
Ductility A_{50mm} (%)	11.2	4.9	5.0	11.6

The MD sheet exhibited the lowest yield and ultimate strengths (about 4-6% lower than the reference blank sheet). Both back-structure Int2.5 and Int12 sheets gave maximally 2% lower strengths as compared to the reference value. Hence, it can be stated that static strength decrease due to micro-drilling application is not very significant.

In case of the ductility, the reference (R) and Int12 back-structure sheets exhibited a twice higher ductility values as compared to MD and Int2.5 configurations. So, LBMD process affects the sheet ductility significantly.

B. Fatigue Tests

The maximum stress value σ_{max} is related to the actual cross-section of the specimen (MD holes were not taken into account for cross-section area calculations). The results in a graphical form (σ_{max}-N_f dependence) are presented in semi-logarithmic coordinates in Fig. 6. Fatigue limit 580 MPa of the reference blank sheet corresponds to 58% value of the static strength. The micro-drilling process results in a significantly lower fatigue life as compared to the reference sheet. There is not a significant difference between the MD and Int2.5 sheets from the fatigue behaviour point of view with only 26-28% fatigue limit as compared to the reference sheet value. Displacement of the back-structure sheet from 2.5 to 12 mm below the MD sheet results in improved fatigue behaviour of perforated sheet (approximately twice maximum stress for the same fatigue life value) with the fatigue limit of 285 MPa (49% of the reference sheet fatigue limit).

C. Fractography

Fractographic analyses of selected fatigue specimens after testing were performed in order to determinate the crack initiation site and direction of the crack propagation in the failure area. The failure of the reference specimens always initiated at the edge corner of the specimen cross-section. The final fracture area forms a majority part of the surface fracture.

Overview and detailed micrographs of the fracture surface examples of typical MD, Int2.5 and Int12 specimens are shown in Figs. 7-9. Always, two overview pictures (from top and side views) and details (showing crack origin sites and micro-fractographic features such as striations, ratcheting marks, ductile dimples, etc.) of the fracture surface are presented.

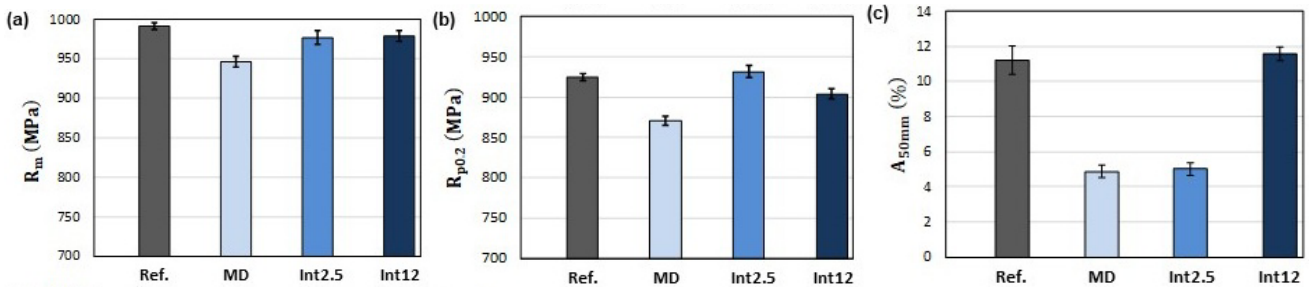


Fig. 5 Tensile test results summary: (a) ultimate strength, (b) yield strength, and (c) ductility comparison

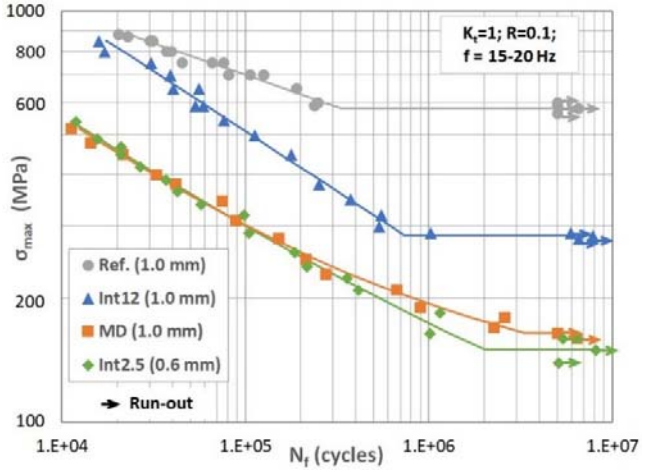


Fig. 6 Fatigue test results comparison

In the overview micrographs, the fatigue crack growth direction is marked using white arrows, and the boundaries between the fatigue and final failure areas are designated with a white dotted line.

The failures of the specimens taken from the MD sheet initiated at the first drilled hole from the edge corner of the specimen's cross-section. Multiple crack initiation could be always observed at the MD holes with present typical ratchet marks when the initiated microcracks interlink together in one major crack. The final fracture area increases with increasing maximum stress level (and decreasing fatigue life). Number of holes where the secondary cracks initiate also rises with increasing maximum stress level. Typical connection sites of two opposing crack fronts are shown in detail in Fig. 7 (the left bottom micrograph).

The failures of the specimens taken from the back-structure sheet Int2.5 (placed in 2.5 mm distance behind the MD sheet) initiated at the first drilled hole from the edge corner of the specimen's cross-section (similarly to the MD batch specimens), see Fig. 8. At the crack origin site, multiple initiations could be always observed along the MD holes (with

typical ratchet marks). Similarly to the MD batch specimens, the final fracture area increases with increasing maximum stress level (and decreasing fatigue life). Nevertheless, in contrast to the MD batch specimens, the holes did not go through the sheet thickness in case of the Int2.5 specimens.

The failures of the specimens taken from the farther back-structure sheet (placed in 12 mm distance behind the MD sheet) initiated at the laser affected sheet surface of the specimen (Fig. 9). The crack initiation occurred in a heat affected zone near the laser or melt material drop interaction spot. At higher loading levels, more initiation sites of secondary cracks were observed at the sheet surface and also in different laser damage spot rows (Fig. 9). Similarly, to other sheets, the fatigue crack growth area increases with decreasing maximum stress level (and increasing fatigue life). In contrast to the closer back-structure Int2.5 sheet specimens, there are no holes in the sheet in case of the Int12 specimens.

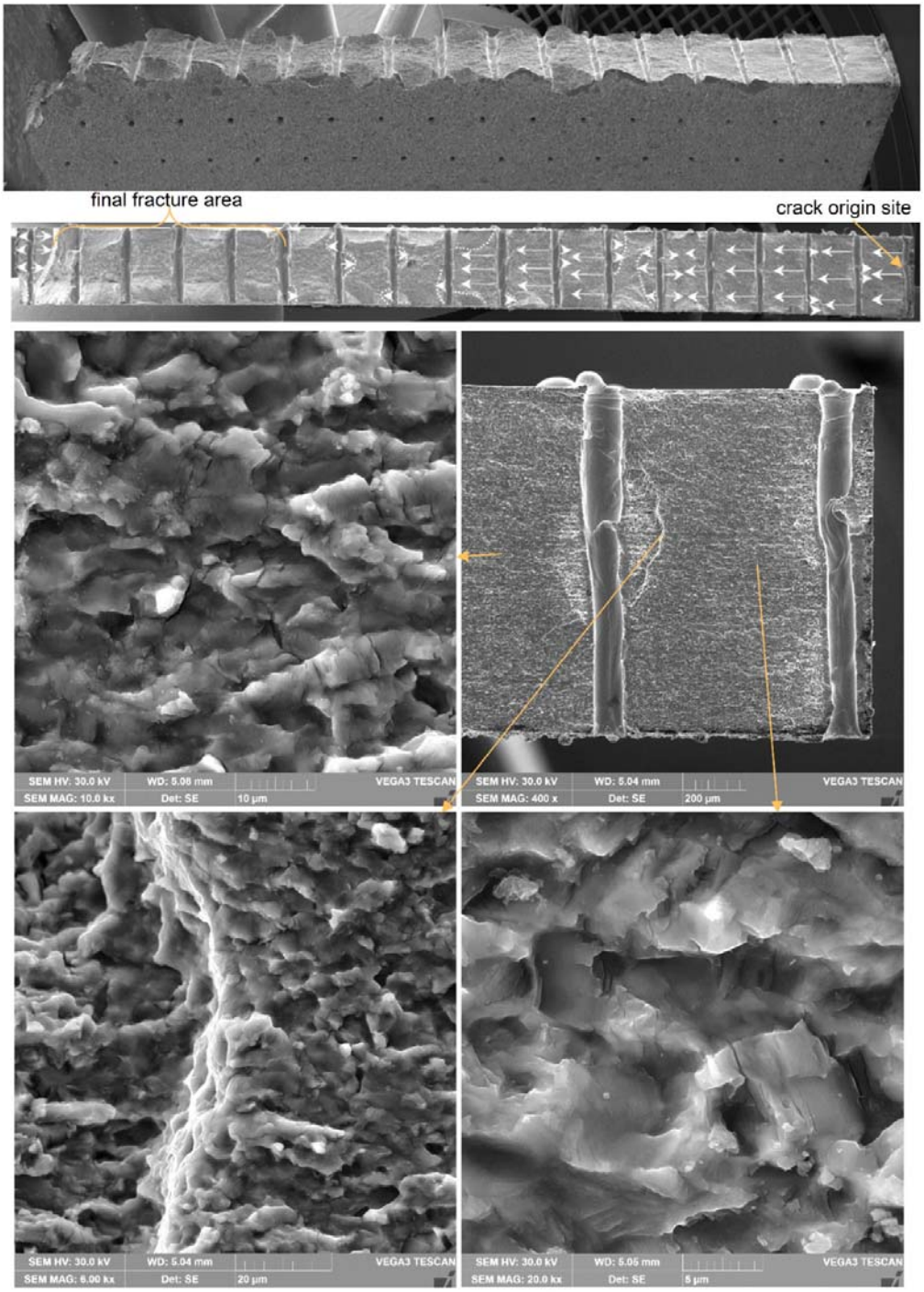


Fig. 7 Overview (crack growth direction marked) and detailed micrographs of the fracture surface – MD specimen (74 360 cycles; σ_{max} = 345 MPa), SEM – various magnification

Open Science Index, Aerospace and Mechanical Engineering Vol:12, No:8, 2018 publications.waset.org/10009330/pdf

Open Science Index, Aerospace and Mechanical Engineering Vol:12, No:8, 2018 publications.waset.org/10009330/pdf

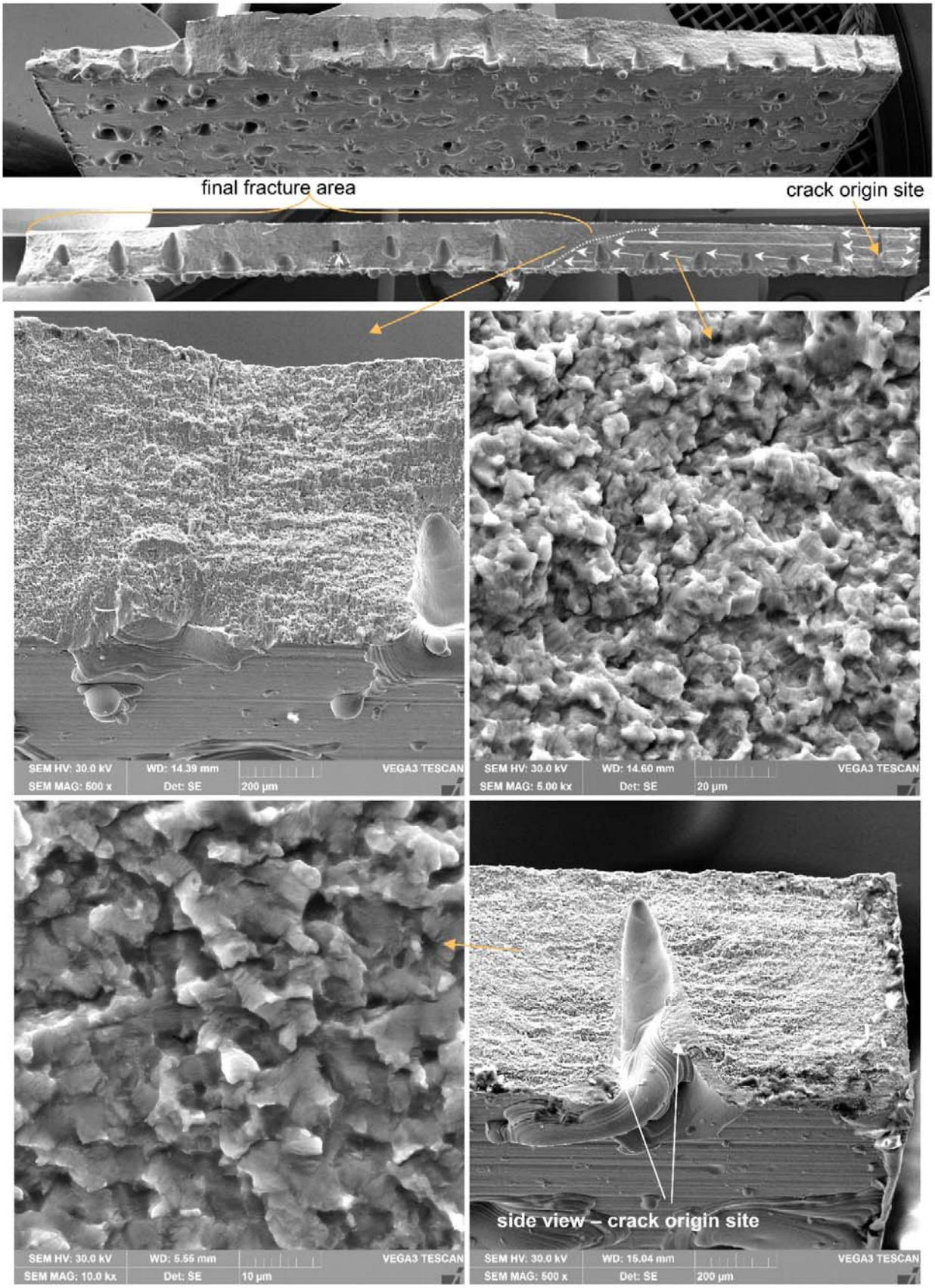


Fig. 8 Overview (crack growth direction marked) and detailed micrographs of the fracture surface – Int2.5 specimen (97 865 cycles; σ_{max} = 320 MPa), SEM – various magnification

Open Science Index, Aerospace and Mechanical Engineering Vol:12, No:8, 2018 publications.waset.org/10009330/pdf

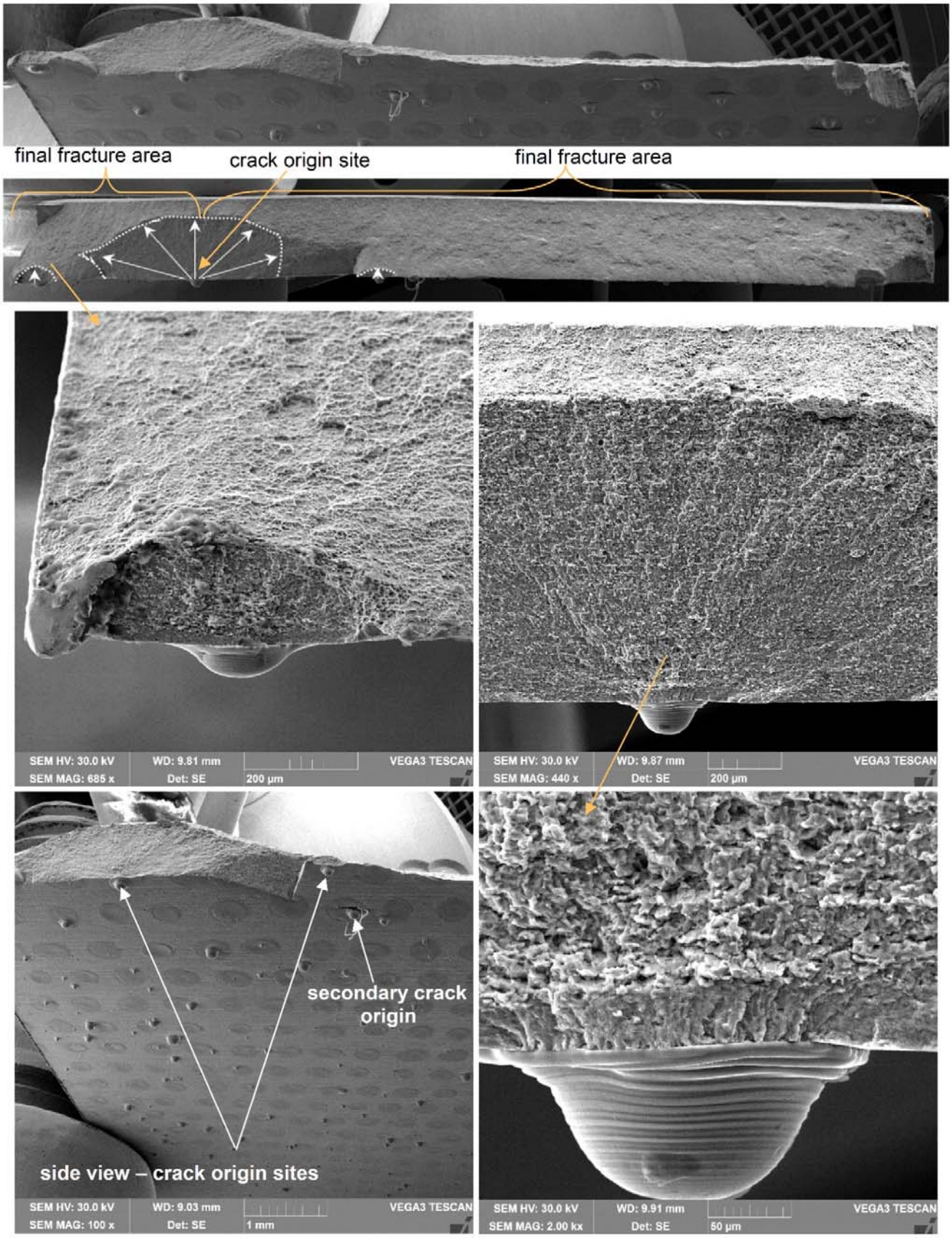


Fig. 9 Overview (crack growth direction marked) and detailed micrographs of the fracture surface – Int12 specimen (15 782 cycles; σ_{max} = 850 MPa), SEM – various magnification

Open Science Index, Aerospace and Mechanical Engineering Vol:12, No:8, 2018 publications.waset.org/10009330/pdf

IV. Conclusion

Knock-down effect of LBMD processing on Ti-6Al-4V (Grade 5) titanium alloy sheets properties was assessed within the AFLoNEXT European project aimed to prove the engineering feasibility of the HLFC technology for drag reduction on fin in flight test and on wing by means of large scale testing.

Two various process configurations were verified with a focus on laser damages in back-structure parts affected by the process. The effects of the LBMD on the material properties were assessed by means of tensile and fatigue tests and fracture surface analyses. The results of this investigation could be summarized as follows:

- Static strength decrease due to micro-drilling application is not very significant (from 2 to 6 %). In case of the ductility, the reference (R) and Int12 back-structure sheets exhibited a twice higher ductility values as compared to MD and Int2.5 configurations.
- The micro-drilling process results in a significantly lower fatigue life (down to 26 %) as compared to the reference sheet.
- Displacement of the back-structure sheet from 2.5 to 12 mm below the MD sheet results in improved fatigue behaviour of perforated sheet (approximately twice maximum stress for the same fatigue life value).
- The failures of the specimens taken from the MD sheet and the back-structure sheet placed in 2.5 mm distance behind the MD sheet initiated at the first drilled hole from the edge corner of the specimen's cross-section.
- The failures of the specimens taken from the farther back-structure sheet (placed in 12 mm distance bellow the MD sheet) initiated at the laser affected sheet surface of the specimen near the laser or melt material drop interaction spot.

It could be summarized that LBDM process applied on the Ti-6Al-4V titanium alloy affects especially the fatigue properties of the sheets, but the fatigue curves give approximately twice longer durability compared with aluminium alloy sheets typically used in airframe structures [5]. Moreover, this implies an application of higher load levels in comparison with aluminium alloys. The specific Aflonext GBD HLFC panel design and its stress level are compatible with the identified allowable, however another geometrical configuration should be carefully checked for its particular reserve factors.

Acknowledgment

The research leading to these results has received funding from the European Union's Seventh Programme for research, technological development and demonstration under grant agreement No 604013. The partners from SONACA (Belgium) are acknowledged for development and performing the LBMD processing.

References

[1] AFLoNEXT (2nd Generation Active Wing - Active Flow, Loads & Noise control on next generation wing) 7P European project No. 604013, http://www.aflonext.eu/.
[2] http://www.aflonext.eu/files/final%20brochure/AFLoNext_Final_Brochure_April2018.pdf.
[3] ISO 6892-1:2016, Metallic materials -- Tensile testing -- Part 1: Method of test at room temperature, July 2016.
[4] EN 6072, Aerospace series - Metallic materials - Test methods - Constant amplitude fatigue testing, 2010.
[5] M. Kadlec, I. Mlch, R. Růžek, "Fatigue Behaviour of Bolted Joints without Load Transfer," in EAN 2017 Conference on Experimental Stress Analysis, Slovakia; 2017, pp. 505-508, EID 2-s2.0-85026312595.